Resubmitted to International Journal of Engineering Science in March 2018

Singularity of subsonic and transonic crack propagations along interfaces of magnetoelectroelastic bimaterials

Abstract

The unified method for addressing the propagation of subsonic and transonic cracks along the interfaces of anisotropic bimaterials in Shen and Nishioka (2000) is applied in this paper for the plain strain problem of subsonic and transonic crack propagation along the interfaces of anisotropic magnetoelectroelastic (MEE) bimaterials. Using a modified Eshelby–Stroh formalism and analytic continuation, the problem here leads to a Riemann–Hilbert problem. After solving the Riemann–Hilbert equation, near-tip asymptotic fields are obtained, which shows the properties of the subsonic and transonic crack propagation in an MEE bimaterial system. Finally, the numerical results related to different singularity powers of the crack-tip are presented and discussed for barium titanate-cobalt ferrite ($BaTiO_3$-$CoFe_2O_4$) composites. The effects of piezoelectricity and piezomagnetics are also examined.

Keywords: Dynamic fractures; MEE bimaterial; Interface crack; subsonic propagation; transonic propagation; crack-tip singularity

1. Introduction

Magnetoelectroelastic (MEE) laminated composites are now being applied as the core components of multifunctional magnetoelectric (ME) energy conversion devices and surface acoustic wave (SAW) devices because of the effects of their unique magneto-electro-elastic

coupling. However, these MEE materials are usually subjected to dynamic loading during their service life which results in interface cracking, one of the most commonly observed failure modes.

In contrast to static fractures (Gao and Noda, 2004; Li and Kardomateas, 2007; Huang et al., 2009; Feng et al., 2010, 2012; Herrmann et al., 2010; Ma et al., 2013, 2015 and 2016), dynamic cracks and their propagation along an interface are more realistic; for example, in transient response and moving crack problems. Zhong et al. (2009) performed a fracture analysis of two limited permeable collinear cracks in a homogeneous MEE body subjected to impact loadings to examine the transient response of in-plane deformation. Chen (2009) established a dynamic contour integral for cracks in magneto-electro-thermo-elastic (METE) materials, and pointed out that the dynamic contour integral could be applied as a physically sound criterion for dynamic fracture analysis. Hu and Chen (2012) considered a pre-existing curving crack problem for an MEE strip under impact loadings and obtained the hoop stress intensity factor. Feng et al. (2009) investigated the transient response of a crack on the interface between two MEE layers.

Another important topic in dynamic fracture mechanics is the moving crack problem (Yoffe, 1951). Some researchers have extended the moving crack model to the analysis of the fracture behaviors of MEE bimaterials (Zhong and Li, 2006; Chen et al., 2012; Hu et al., 2015), but only considered the anti-plane state. Among them, Zhong and Li (2006) studied a moving Yoffe crack of the interfaces between two types of MEE bimaterials based on the ME boundary conditions of a limited permeable crack-face. Chen et al. (2012) considered the problem of the propagation of a semi-infinite interfacial crack between piezoelectric and piezomagnetic solids. They observed that when determining the dynamic fracture parameters, the B-G waves play an important role for the considered combination of materials. Using the Fourier-transform method, Hu et al. (2015) investigated a moving ME permeable crack at the interfaces of MEE bimaterials by using the

Dugdale model. They concluded that the generalized stresses are no longer singular at the crack tip. For in-plane fracture problems, Ma et al. (2017) analyzed the fracture behavior of a moving interface crack with a contact zone between two dissimilar types of MEE materials. They examined the effect of the speed of the moving crack, poling direction, material volume fraction, load position and load ratio on the fracture parameters. However, their work is only limited to the subsonic regime.

A comprehensive review regarding steady-state and transient problems for uniform and non-uniform plane crack propagation in an homogeneous elastic solid can be found in Slepyan (2002), in which the speed-dependent crack-tip asymptotic fields were presented for different speed regions, including sub-Rayleigh, super-Rayleigh, transonic and supersonic regimes. Moreover, it was shown that, as a macrolevel crack growth criterion, the principle of maximum energy dissipation rate (Slepyan, 1993) could satisfactorily predict the propagation behavior of the dynamic cracks in brittle materials. On the other hand, investigations on transonic crack propagation in bimaterials can be traced back to Yang et al. (1991) and Liu et al. (1993), and continued by other researchers, such as Lambros and Rosakis (1995), Yu and Yang (1995), Huang et al. (1996), and Nishioka and Yasin (1999). Yang et al. (1991) first proposed the theoretical possibility of transonic crack growth in elastic bimaterials. Liu at al. (1993) and Lambros and Rosakis (1995) observed that the speed of the crack-tip could be faster than the minimum shear wave speed of the poly(methyl methacrylate) (PMMA)/steel bimaterial system in their experimental investigation. Liu et al. (1995) pointed out that the near-tip field of transonic crack propagation at the interface of bimaterials is shear dominated and large scale contact could develop behind the crack tip for a certain velocity range. Yu and Yang (1995) and Huang et al. (1996) presented an asymptotic solution for a transonic crack at the isotropic bimaterial interface and demonstrated that a Mach wave emanates from the crack tip. Nishioka and Yasin (1999)

performed simulations of the propagation of subsonic, transonic and supersonic cracks at the interfaces between isotropic bimaterials subjected to tension and shear dominated loadings, respectively. Their results showed that in the supersonic regime, the dynamic energy release rate is always equal to zero. Rosakis et al. (1998) further confirmed the possibility of supersonic crack growth based on experiments. Samudrala and Rosakis (2003) studied the effects of loading and geometry on the subsonic/transonic transition of a crack at a bimaterial interface. They showed that the formation, size and evolution of the contact zone substantially differ based on the sign of the opening component of loading. Taking into account the effects of contact, Huang et al. (1998) and Wang et al. (1998) proposed near-tip solutions of a transonic crack at the interface between elastic/rigid and elastic/elastic bimaterials. On the other hand, Xu and Needleman (1996), Needleman and Rosakis (1999) and Hao et al. (2004) examined transonic crack growth of bimaterial debonding by using numerical simulation and also observed that compressive normal stresses along part of the interface could lead to the development of a large contact zone length. More recently, Barras et al. (2014) numerically investigated the in-plane propagation of bimaterial interfaces by considering the frictional contact with a spectral formulation of elastodynamic boundary integral equations.

However, all of these aforementioned works that concern interface crack propagation in a transonic regime are limited to isotropic bimaterial systems. Shen and Nishioka (2000) and Shen et al. (2000), respectively, considered the singularity of subsonic and transonic crack propagations along anisotropic elastic and piezoelectric bimaterials by using a unified method. They found that a Mach wave emanates from the crack tip and moves with the crack tip when the crack propagates in a transonic regime. Wu (2002) presented the crack-tip field of a supersonic crack at the interface of anisotropic bimaterials. However, to the best of the knowledge of the authors, the singularity of subsonic and transonic crack propagation along the interfaces of MEE

bimaterials has not been reported yet. Therefore, in this paper, we discuss the asymptotic structure of the crack-tip field of a moving crack in the subsonic and transonic regimes at the interfaces of MEE bimaterials by referring to the unified method proposed by Shen and Nishioka (2000). Using modified Eshelby–Stroh formalism and analytic continuation, the problem here leads to a Riemann–Hilbert problem. After solving the Riemann–Hilbert equation, the near-tip asymptotic fields are obtained, which show the properties of the subsonic and transonic crack propagation in an MEE bimaterial system. Finally, the numerical results related to the singularity powers of the crack-tip are presented for barium titanate-cobalt ferrite ($BaTiO_3$-$CoFe_2O_4$) composites in order to show the fracture properties of the asymptotic fields.

2. Basic relations for MEE bimaterials with moving coordinate system

According to Huang et al. (1997), the dynamic constitutive equations for an MEE solid in a fixed coordinate system (X_1, X_2, X_3) can be written in the forms of:

$$\begin{cases} \sigma_{ij} = c_{ijkl}u_{k,l} - e_{lij}\varphi_{,l} - h_{lij}\phi_{,l} \\ D_i = e_{ikl}u_{k,l} + \alpha_{il}\varphi_{,l} + d_{il}\phi_{,l} \\ B_i = h_{ikl}u_{k,l} + d_{il}\varphi_{,l} + \mu_{il}\phi_{,l} \end{cases} \tag{1}$$

$$\begin{cases} \left(c_{ijkl}u_k + e_{lij}\varphi + h_{lij}\phi\right)_{,li} = \rho\dfrac{\partial^2 u_j}{\partial t^2} \\ \left(e_{ikl}u_k - \alpha_{il}\varphi - d_{il}\phi\right)_{,li} = 0 \\ \left(h_{ikl}u_k - d_{il}\varphi - \mu_{il}\phi\right)_{,li} = 0 \end{cases} \tag{2}$$

where σ_{ij}, D_i, and B_i are the components of the stresses, electric displacements and magnetic inductions, respectively; u_i, φ, and ϕ are the mechanical displacement components, and electric and magnetic potentials, respectively. c_{ijkl}, e_{ikl}, h_{ikl}, and d_{il} are the elastic, piezoelectric, piezomagnetic, and electromagnetic constants, respectively; α_{il}, μ_{li} are the dielectric

permittivities and magnetic permeabilities, respectively, and ρ is the material density. i, j, k, s range in $\{1,2,3\}$, the repeated indexes imply summation, and the comma stands for the differentiation with respect to the corresponding coordinate variables.

In this study, we consider the in-plane fracture problem of monoclinic MEE materials with a symmetry plane at $X_2 = 0$ in the absence of body force, electric charge and electric current, in which all the fields are independent of the coordinate $X_2 = 0$, and the displacement u_2 decouples in the (X_1, X_3)-plane from the components $\mathbf{U} = \{u_1,\ u_3,\ \varphi,\ \phi\}^{\mathrm{T}}$. The following conditions for the material constants in contracted notation are satisfied in this case (Li and Kardomateas, 2007):

$$c_{14} = c_{16} = c_{34} = c_{36} = c_{54} = c_{56} = 0,\ e_{14} = e_{16} = e_{34} = e_{36} = 0,\ h_{14} = h_{16} = h_{34} = h_{36} = 0 \tag{3}$$

Assuming that the crack moves along the material interfaces, the following coordinate transformation is performed $x_1 = X_1 - vt$, $x_2 = X_2$, $x_3 = X_3$, where v is the speed of the crack tip. In the moving coordinate system, Eq. (2) can be rewritten as:

$$\mathbf{Q}\mathbf{U}_{,11} + \left(\mathbf{R} + \mathbf{R}^{\mathrm{T}}\right)\mathbf{U}_{,13} + \mathbf{T}\mathbf{U}_{,33} = 0 \tag{4}$$

where

$$\mathbf{Q} = \begin{pmatrix} \mathbf{Q}_0 & \mathbf{e}_{11} & \mathbf{h}_{11} \\ \mathbf{e}_{11}^{\mathrm{T}} & -\alpha_{11} & -d_{11} \\ \mathbf{h}_{11}^{\mathrm{T}} & -d_{11} & -\mu_{11} \end{pmatrix},\ \mathbf{R} = \begin{pmatrix} \mathbf{R}_0 & \mathbf{e}_{31} & \mathbf{h}_{31} \\ \mathbf{e}_{13}^{\mathrm{T}} & -\alpha_{13} & -d_{13} \\ \mathbf{h}_{13}^{\mathrm{T}} & -d_{13} & -\mu_{13} \end{pmatrix},\ \mathbf{T} = \begin{pmatrix} \mathbf{T}_0 & \mathbf{e}_{33} & \mathbf{h}_{33} \\ \mathbf{e}_{33}^{\mathrm{T}} & -\alpha_{33} & -d_{33} \\ \mathbf{h}_{33}^{\mathrm{T}} & -d_{33} & -\mu_{33} \end{pmatrix} \tag{5a}$$

$$\left(\mathbf{Q}_0\right)_{jk} = c_{1jk1} - \rho v^2 \delta_{jk},\ \left(\mathbf{R}_0\right)_{jk} = c_{1jk3},\ \left(\mathbf{T}_0\right)_{jk} = c_{3jk3},\ (\mathbf{e}_{ij})_m = e_{ijm},\ (\mathbf{h}_{ij})_m = h_{ijm} \tag{5b}$$

and δ_{jk} is the Kronecker delta.

By using and applying the Lekhnitskii–Eshelby–Stroh representation to MEE materials, a general solution from Eq. (4) can be presented in the form (Gao and Noda, 2004):

$$\mathbf{U} = \sum_{s=\pm 1}^{\pm 4} \mathbf{A}_s f_s\left(z_s, t\right) \tag{6}$$

$$\mathbf{t} = \sum_{s=\pm 1}^{\pm 4} \mathbf{B}_s f_s'\left(z_s, t\right) \tag{7}$$

where $\mathbf{U} = \left\{u_1,\ u_3,\ \varphi,\ \phi\right\}^{\mathrm{T}}$, $\mathbf{t} = \left\{\sigma_{31},\ \sigma_{33},\ D_3,\ B_3\right\}^{\mathrm{T}}$ (the superscript 'T' stands for the transposed matrix), $\mathbf{A} = \left\{\mathbf{A}_1,\ \mathbf{A}_2,\ \mathbf{A}_3,\ \mathbf{A}_4\right\}^{\mathrm{T}}$; $f_s\left(z_s\right)$ in Eqs. (6) and (7) is an arbitrary analytic function with $z_s = x_1 + p_s x_3 \left(s = \pm 1, \pm 2, \pm 3, \pm 4\right)$. For a fixed s, p_s and $\mathbf{A}_s = \left\{a_{1s},\ a_{2s},\ a_{3s},\ a_{4s}\right\}^{\mathrm{T}}$ are respectively an eigenvalue and an eigenvector of the system.

$$\left\{\mathbf{Q} + p_s\left(\mathbf{R} + \mathbf{R}^{\mathrm{T}}\right) + p_s^2 \mathbf{T}\right\}\mathbf{A}_s = 0 \tag{8}$$

The 4×4 matrix $\mathbf{B}$ can be obtained with the formula $\mathbf{B} = \mathbf{R}^{\mathrm{T}}\mathbf{A} + \mathbf{TAP}$ with $\mathbf{P} = \mathrm{diag}\left\{p_1,\ p_2,\ p_3,\ p_4\right\}$. The prime $\left(\prime\right)$ denotes differentiation with respect to the argument, and the overbar stands for the complex conjugate.

It is noted that $\mathbf{A}_s$ is real when p_s is real, and $\mathbf{A}_s$ and $\mathbf{A}_{-s}$ are complex conjugates when $\mathbf{A}_s$ is complex. A positive value of s corresponds to the root p_s with a positive imaginary part. If real roots exist, then the positive value of s is designated as the root which produces a positive factor $\mathbf{A}_s^{\mathrm{T}}\mathbf{B}_s$. The terms with a real p_s and positive s represent the enthalpy flow in the positive x_3 direction (Shen and Nishioka, 2000).

The general solution in Eq. (6) depends on whether the roots p_s are real or complex. When $v = 0$ all p_s are complex. In this work, the in-plane deformation decouples from the out-plane deformation and we only consider that the p_s are real. Therefore, there are only two critical values of v, where a pair of roots p_{i+1} and $p_{-(i+1)}$ changes from complex to real. Take i such that

$$v_1 \geq v_2 > 0 \tag{9}$$

If $v < v_2$, then the roots p_s are all complex. The motion may be described as subsonic. If $v > v_2$, then at least two roots p_4 and p_{-4} are real, and the motion will be accompanied with the generation of waves. At any of the two critical velocities v_i, the two roots p_{i+1} and $p_{-(i+1)}$ are necessarily equal and the solution for **U** will require further special consideration (Shen et al., 2000).

If $v > v_2$, then at least $f_4\left(z_4\right)$ and $f_{-4}\left(z_{-4}\right)$ are real functions of their respective arguments. Similar to the supersonic flow in aerodynamics, the point ahead of the crack tip in crack propagation is damaged by the moving supersonic crack, and hence (Shen et al., 2000):

$$\begin{cases} f_{-4}\left(z_{-4}\right) = 0 & \text{for } x_3 > 0 \\ f_4\left(z_4\right) = 0 & \text{for } x_3 < 0 \end{cases} \tag{10}$$

3. Crack-tip fields of cracks at interface

Consider an anisotropic MEE bimaterial system in a fixed rectangular coordinate system. Materials 1 and 2 correspond to $x_3 > 0$ and $x_3 < 0$, respectively. Let $v_2^{(1)} < v_2^{(2)}$. The crack moves along the interfaces of the materials at a constant speed v and the growth is assumed to be constant. In the moving coordinate $\left(x_1,\ x_3\right)$, a semi-infinite crack is located in $x_1 < 0$ and $x_3 = 0$. The velocity range is limited to $0 \le v < \min\left(v_1^{(1)}, v_1^{(2)}\right)$. Hence, the crack propogation is subsonic or transonic.

Assume that:

$$m = \begin{cases} 0, & \text{for } 0 \le v < v_2^{(1)} \\ 1, & \text{for } v_2^{(1)} < v < \min\left(v_1^{(1)}, v_2^{(2)}\right) \\ 2, & \text{for } v_1^{(1)} < v < \min\left(v_1^{(1)}, v_2^{(2)}\right) \end{cases} \tag{11}$$

According to Eq.(10), Eqs. (6) and (7) can be written as:

$$\mathbf{U} = 2\,\mathrm{Re}\sum_{s=1}^{4}\mathbf{A}_s f_s\left(z_s,t\right) \tag{12}$$

$$\mathbf{t} = 2\,\mathrm{Re}\sum_{s=1}^{4}\mathbf{B}_s f_s'\left(z_s,t\right) \tag{13}$$

where Re denotes the real part, and $f_s\left(z_s,t\right)$ is analytic in its arguments when it is complex, or is a real function of its arguments when it is real.

Now, the general solution can be further written as:

$$\mathbf{U}^{(1)} = \begin{bmatrix}\mathbf{A}_{11}^{(1)} & \mathbf{A}_{12}^{(1)}\\ \mathbf{A}_{21}^{(1)} & \mathbf{A}_{22}^{(1)}\end{bmatrix}\begin{bmatrix}\mathbf{f}_1^{(1)}\left(z\right)\\ \mathbf{f}_2^{(1)}\left(z\right)\end{bmatrix} + \begin{bmatrix}\overline{\mathbf{A}}_{11}^{(1)} & \mathbf{A}_{12}^{(1)}\\ \overline{\mathbf{A}}_{21}^{(1)} & \mathbf{A}_{22}^{(1)}\end{bmatrix}\begin{bmatrix}\overline{\mathbf{f}}_1^{(1)}\left(z\right)\\ \mathbf{f}_2^{(1)}\left(z\right)\end{bmatrix} \tag{14}$$

$$\mathbf{U}^{(2)} = \begin{bmatrix}\mathbf{A}_{11}^{(2)} & \mathbf{A}_{12}^{(2)}\\ \mathbf{A}_{21}^{(2)} & \mathbf{A}_{22}^{(2)}\end{bmatrix}\begin{bmatrix}\mathbf{f}_1^{(2)}\left(z\right)\\ \mathbf{f}_2^{(2)}\left(z\right)\end{bmatrix} + \begin{bmatrix}\overline{\mathbf{A}}_{11}^{(2)} & \overline{\mathbf{A}}_{12}^{(2)}\\ \overline{\mathbf{A}}_{21}^{(2)} & \overline{\mathbf{A}}_{22}^{(2)}\end{bmatrix}\begin{bmatrix}\overline{\mathbf{f}}_1^{(2)}\left(z\right)\\ \overline{\mathbf{f}}_2^{(2)}\left(z\right)\end{bmatrix} \tag{15}$$

and

$$\mathbf{t}^{(1)} = \begin{bmatrix}\mathbf{B}_{11}^{(1)} & \mathbf{B}_{12}^{(1)}\\ \mathbf{B}_{21}^{(1)} & \mathbf{B}_{22}^{(1)}\end{bmatrix}\begin{bmatrix}\mathbf{f}_1'^{(1)}\left(z\right)\\ \mathbf{f}_2'^{(1)}\left(z\right)\end{bmatrix} + \begin{bmatrix}\overline{\mathbf{B}}_{11}^{(1)} & \mathbf{B}_{12}^{(1)}\\ \overline{\mathbf{B}}_{21}^{(1)} & \mathbf{B}_{22}^{(1)}\end{bmatrix}\begin{bmatrix}\overline{\mathbf{f}}_1'^{(1)}\left(z\right)\\ \mathbf{f}_2'^{(1)}\left(z\right)\end{bmatrix} \tag{16}$$

$$\mathbf{t}^{(2)} = \begin{bmatrix}\mathbf{B}_{11}^{(2)} & \mathbf{B}_{12}^{(2)}\\ \mathbf{B}_{21}^{(2)} & \mathbf{B}_{22}^{(2)}\end{bmatrix}\begin{bmatrix}\mathbf{f}_1'^{(2)}\left(z\right)\\ \mathbf{f}_2'^{(2)}\left(z\right)\end{bmatrix} + \begin{bmatrix}\overline{\mathbf{B}}_{11}^{(2)} & \overline{\mathbf{B}}_{12}^{(2)}\\ \overline{\mathbf{B}}_{21}^{(2)} & \overline{\mathbf{B}}_{22}^{(2)}\end{bmatrix}\begin{bmatrix}\overline{\mathbf{f}}_1'^{(2)}\left(z\right)\\ \mathbf{f}_2'^{(2)}\left(z\right)\end{bmatrix} \tag{17}$$

where $\mathbf{A}_{22}^{(1)}$, $\mathbf{A}_{12}^{(1)}$, $\mathbf{B}_{22}^{(1)}$, $\mathbf{B}_{12}^{(1)}$ and $\mathbf{f}_2^{(1)}\left(z\right)$ are real and

$$\mathbf{A} = \begin{bmatrix}\mathbf{A}_1 & \mathbf{A}_2 & \mathbf{A}_3 & \mathbf{A}_4\end{bmatrix} = \begin{bmatrix}\mathbf{A}_{11} & \mathbf{A}_{12}\\ \mathbf{A}_{21} & \mathbf{A}_{22}\end{bmatrix} \tag{18}$$

$$\mathbf{B} = \begin{bmatrix}\mathbf{B}_1 & \mathbf{B}_2 & \mathbf{B}_3 & \mathbf{B}_4\end{bmatrix} = \begin{bmatrix}\mathbf{B}_{11} & \mathbf{B}_{12}\\ \mathbf{B}_{21} & \mathbf{B}_{22}\end{bmatrix} \tag{19}$$

It should be noted that $\mathbf{A}_{11}$ is a $\left(4-m\right)\times\left(4-m\right)$ submatrix of $\mathbf{A}$, $\mathbf{A}_{12}$ is a $\left(4-m\right)\times m$ submatrix of $\mathbf{A}$, $\mathbf{A}_{21}$ is a $m\times\left(4-m\right)$ submatrix of $\mathbf{A}$, and $\mathbf{A}_{12}$ is a $\left(4-m\right)\times m$ submatrix of $\mathbf{A}$. This is

also the same for $\mathbf{B}_{ij}$ of $\mathbf{B}$. $\mathbf{f}_1(z)$ is a $(4-m)$-component column and $\mathbf{f}_2(z)$ is an m-component column. Both $\mathbf{A}$ and $\mathbf{B}$ are nonsingular (v does not take the Rayleigh wave speed of either substrate or v_i). The bimaterial matrix is defined as:

$$\mathbf{H} = \mathbf{Y}^{(1)} + \overline{\mathbf{Y}}^{(2)} \tag{20}$$

where $\mathbf{Y} = \mathrm{i}\mathbf{A}\mathbf{B}^{-1}$ is a Hermitian matrix for $0 \le v < v_2$. The matrix $\mathbf{H}$ characterizes the interface and propagation behavior.

For $x_1 > 0$, the continuity of the generalized displacements across the interface leads to

$$2\mathbf{A}_{12}^{(1)}\mathbf{f}_2^{(1)}(x_1) + \mathbf{A}_{11}^{(1)}\mathbf{f}_1^{(1)}(x_1) + \overline{\mathbf{A}}_{11}^{(1)}\overline{\mathbf{f}}_1^{(1)}(x_1) = \mathbf{A}_{11}^{(2)}\mathbf{f}_1^{(2)}(x_1) + \mathbf{A}_{12}^{(2)}\mathbf{f}_2^{(2)}(x_1) + \overline{\mathbf{A}}_{11}^{(2)}\overline{\mathbf{f}}_1^{(2)}(x_1) + \overline{\mathbf{A}}_{12}^{(2)}\overline{\mathbf{f}}_2^{(2)}(x_1) \tag{21}$$

and

$$2\mathbf{A}_{22}^{(1)}\mathbf{f}_2^{(1)}(x_1) + \mathbf{A}_{21}^{(1)}\mathbf{f}_1^{(1)}(x_1) + \overline{\mathbf{A}}_{21}^{(1)}\overline{\mathbf{f}}_1^{(1)}(x_1) = \mathbf{A}_{21}^{(2)}\mathbf{f}_1^{(2)}(x_1) + \mathbf{A}_{22}^{(2)}\mathbf{f}_2^{(2)}(x_1) + \overline{\mathbf{A}}_{21}^{(2)}\overline{\mathbf{f}}_1^{(2)}(x_1) + \overline{\mathbf{A}}_{22}^{(2)}\overline{\mathbf{f}}_2^{(2)}(x_1) \tag{22}$$

For $x_1 > 0$, the continuity of the generalized stresses across the interface leads to

$$2\mathbf{B}_{12}^{(1)}\mathbf{f}_2'^{(1)}(x_1) + \mathbf{B}_{11}^{(1)}\mathbf{f}_1'^{(1)}(x_1) + \overline{\mathbf{B}}_{11}^{(1)}\overline{\mathbf{f}}_1'^{(1)}(x_1) = \mathbf{B}_{11}^{(2)}\mathbf{f}_1'^{(2)}(x_1) + \mathbf{B}_{12}^{(2)}\mathbf{f}_2'^{(2)}(x_1) + \overline{\mathbf{B}}_{11}^{(2)}\overline{\mathbf{f}}_1'^{(2)}(x_1) + \overline{\mathbf{B}}_{12}^{(2)}\overline{\mathbf{f}}_2'^{(2)}(x_1) \tag{23}$$

and

$$2\mathbf{B}_{22}^{(1)}\mathbf{f}_2'^{(1)}(x_1) + \mathbf{B}_{21}^{(1)}\mathbf{f}_1'^{(1)}(x_1) + \overline{\mathbf{B}}_{21}^{(1)}\overline{\mathbf{f}}_1'^{(1)}(x_1) = \mathbf{B}_{21}^{(2)}\mathbf{f}_1'^{(2)}(x_1) + \mathbf{B}_{22}^{(2)}\mathbf{f}_2'^{(2)}(x_1) + \overline{\mathbf{B}}_{21}^{(2)}\overline{\mathbf{f}}_1'^{(2)}(x_1) + \overline{\mathbf{B}}_{22}^{(2)}\overline{\mathbf{f}}_2'^{(2)}(x_1) \tag{24}$$

Using Eqs.(21)-(24) and eliminating $\mathbf{f}_2'^{(1)}(x_1)$ provide:

$$\mathbf{M}\begin{bmatrix}\mathbf{f}_1'^{(1)}(x_1)\\ \overline{\mathbf{f}}_1'^{(2)}(x_1)\\ \overline{\mathbf{f}}_2'^{(2)}(x_1)\end{bmatrix} - \overline{\mathbf{M}}\begin{bmatrix}\overline{\mathbf{f}}_1'^{(1)}(x_1)\\ \mathbf{f}_1'^{(2)}(x_1)\\ \mathbf{f}_2'^{(2)}(x_1)\end{bmatrix} = 0 \tag{25}$$

where $\mathbf{M}$ is a $(8-m)\times(8-m)$ matrix and

$$\mathbf{M}=\mathrm{i}\begin{bmatrix} -\mathbf{B}_{12}^{(1)}\left(\mathbf{B}_{22}^{(1)}\right)^{-1}\mathbf{B}_{21}^{(1)}+\mathbf{B}_{11}^{(1)} & \mathbf{B}_{12}^{(1)}\left(\mathbf{B}_{22}^{(1)}\right)^{-1}\overline{\mathbf{B}}_{21}^{(2)}-\overline{\mathbf{B}}_{11}^{(2)} & \mathbf{B}_{12}^{(1)}\left(\mathbf{B}_{22}^{(1)}\right)^{-1}\overline{\mathbf{B}}_{22}^{(2)}-\overline{\mathbf{B}}_{12}^{(2)} \\ -\mathbf{A}_{12}^{(1)}\left(\mathbf{B}_{22}^{(1)}\right)^{-1}\mathbf{B}_{21}^{(1)}+\mathbf{A}_{11}^{(1)} & \mathbf{A}_{12}^{(1)}\left(\mathbf{B}_{22}^{(1)}\right)^{-1}\overline{\mathbf{B}}_{21}^{(2)}-\overline{\mathbf{A}}_{11}^{(2)} & \mathbf{A}_{12}^{(1)}\left(\mathbf{B}_{22}^{(1)}\right)^{-1}\overline{\mathbf{B}}_{22}^{(2)}-\overline{\mathbf{A}}_{12}^{(2)} \\ -\mathbf{A}_{22}^{(1)}\left(\mathbf{B}_{22}^{(1)}\right)^{-1}\mathbf{B}_{21}^{(1)}+\mathbf{A}_{21}^{(1)} & \mathbf{A}_{22}^{(1)}\left(\mathbf{B}_{22}^{(1)}\right)^{-1}\overline{\mathbf{B}}_{21}^{(2)}-\overline{\mathbf{A}}_{21}^{(2)} & \mathbf{A}_{22}^{(1)}\left(\mathbf{B}_{22}^{(1)}\right)^{-1}\overline{\mathbf{B}}_{22}^{(2)}-\overline{\mathbf{A}}_{22}^{(2)} \end{bmatrix} \tag{26}$$

By using analytic continuation, Eq. (25) leads to a new function $\mathbf{h}(z)$ that is analytic in the entire plane except for the crack surface (Shen et al., 2000):

$$\mathbf{h}(z)=\begin{cases}\mathbf{M}\left[\mathbf{f}_1'^{(1)}(z) \quad \overline{\mathbf{f}}'^{(2)}(z)\right]^{\mathrm{T}}, & x_3>0\\ \overline{\mathbf{M}}\left[\overline{\mathbf{f}}_1'^{(1)}(z) \quad \mathbf{f}'^{(2)}(z)\right]^{\mathrm{T}}, & x_3>0\end{cases} \tag{27}$$

Using traction-free conditions on the upper crack surface gives:

$$2\mathbf{B}_{12}^{(1)}\mathbf{f}_2'^{(1)}(x_1)+\mathbf{B}_{11}^{(1)}\mathbf{f}_1'^{(1)}(x_1)+\overline{\mathbf{B}}_{11}^{(1)}\overline{\mathbf{f}}_1'^{(1)}(x_1)=0, \quad \text{for } x_1<0 \tag{28}$$

$$2\mathbf{B}_{22}^{(1)}\mathbf{f}_2'^{(1)}(x_1)+\mathbf{B}_{21}^{(1)}\mathbf{f}_1'^{(1)}(x_1)+\overline{\mathbf{B}}_{21}^{(1)}\overline{\mathbf{f}}_1'^{(1)}(x_1)=0, \quad \text{for } x_1<0 \tag{29}$$

Eliminating $\mathbf{f}_2'^{(1)}(x_1)$ gives:

$$\left[\mathbf{B}_{11}^{(1)}-\mathbf{B}_{12}^{(1)}\left(\mathbf{B}_{22}^{(1)}\right)^{-1}\mathbf{B}_{21}^{(1)}\right]\mathbf{f}_1'^{(1)}(x_1)+\left[\overline{\mathbf{B}}_{11}^{(1)}-\mathbf{B}_{12}^{(1)}\left(\mathbf{B}_{22}^{(1)}\right)^{-1}\overline{\mathbf{B}}_{21}^{(1)}\right]\overline{\mathbf{f}}_1'^{(1)}(x_1)=0, \quad \text{for } x_1<0 \tag{30}$$

Using traction-free conditions on the lower crack surface results in:

$$\mathbf{B}^{(2)}\mathbf{f}'^{(2)}(x_1)+\overline{\mathbf{B}}^{(2)}\overline{\mathbf{f}}'^{(2)}(x_1)=0, \quad \text{for } x_1<0 \tag{31}$$

Combining Eq. (30) with Eq. (31) and using Eq. (27) results in:

$$\mathbf{P}^{-1}\mathbf{h}^{+}(x_1)+\overline{\mathbf{P}}^{-1}\mathbf{h}^{-}(x_1)=0, \quad \text{for } x_1<0 \tag{32}$$

where

$$\mathbf{P}=\mathbf{M}\mathbf{V}^{-1}, \quad \mathbf{V}=\begin{bmatrix}\mathbf{B}_{11}^{(1)}-\mathbf{B}_{12}^{(1)}\left(\mathbf{B}_{22}^{(1)}\right)^{-1}\mathbf{B}_{21}^{(1)} & 0\\ 0 & \overline{\mathbf{B}}^{(2)}\end{bmatrix} \tag{33}$$

The submatrices of $\mathbf{P}$ can be expressed as (Shen et al., 2000):

$$\mathbf{P}_{11}=\mathrm{i}\mathbf{I},\ \mathbf{P}_{12}=\left[-\mathrm{i}\mathbf{I}\quad \mathrm{i}\mathbf{B}_{12}^{(1)}\left(\mathbf{B}_{22}^{(1)}\right)^{-1}\right] \tag{34a}$$

$$\mathbf{P}_{21}=\mathrm{i}\begin{bmatrix}\mathbf{A}_{11}^{(1)}-\mathbf{A}_{12}^{(1)}\left(\mathbf{B}_{22}^{(1)}\right)^{-1}\mathbf{B}_{21}^{(1)}\\ \mathbf{A}_{21}^{(1)}-\mathbf{A}_{22}^{(1)}\left(\mathbf{B}_{22}^{(1)}\right)^{-1}\mathbf{B}_{21}^{(1)}\end{bmatrix}\mathbf{V}_{11}^{-1},\ \mathbf{P}_{22}=\mathrm{i}\begin{bmatrix}0 & \mathbf{A}_{12}^{(1)}\left(\mathbf{B}_{22}^{(1)}\right)^{-1}\\ 0 & \mathbf{A}_{22}^{(1)}\left(\mathbf{B}_{22}^{(1)}\right)^{-1}\end{bmatrix}-\mathrm{i}\overline{\mathbf{A}}^{(2)}\left(\overline{\mathbf{B}}^{(2)}\right)^{-1} \tag{34b}$$

In Eq. (34), the dimensions of the submatrices $\mathbf{P}_{11}$, $\mathbf{P}_{12}$, $\mathbf{P}_{21}$ and $\mathbf{P}_{22}$ are $(4-m)\times(4-m)$, $(4-m)\times 4$, $4\times(4-m)$ and 4×4, respectively.

Here, an auxiliary problem is introduced and solved for Eq. (32). Let λ_i be the eigenvalues and $\mathbf{d}_i$ the corresponding eigenvectors for the eigenvalue problem:

$$\mathbf{P}^{-1}\mathbf{d}+\lambda\overline{\mathbf{P}}^{-1}\mathbf{d}=0 \tag{35}$$

Let $\mathbf{d}=\mathbf{P}\mathbf{g}$, where $\mathbf{g}=\left[\mathbf{g}_1\quad \mathbf{g}_2\right]^{\mathrm{T}}$ is a new vector, $\mathbf{g}_1$ and $\mathbf{g}_2$ are $(4-m)$-component and four-component columns. Eq. (32) can be transformed into a new eigenvalue problem:

$$\left(\lambda\mathbf{P}+\overline{\mathbf{P}}\right)\mathbf{g}=0 \tag{36}$$

Thus,

$$\lambda\left(\mathbf{P}_{11}\mathbf{g}_1+\mathbf{P}_{12}\mathbf{g}_2\right)+\left(\overline{\mathbf{P}}_{11}\mathbf{g}_1+\overline{\mathbf{P}}_{12}\mathbf{g}_2\right)=0 \tag{37}$$

and

$$\lambda\left(\mathbf{P}_{21}\mathbf{g}_1+\mathbf{P}_{22}\mathbf{g}_2\right)+\left(\overline{\mathbf{P}}_{21}\mathbf{g}_1+\overline{\mathbf{P}}_{22}\mathbf{g}_2\right)=0 \tag{38}$$

Using Eqs. (34) and (37) results in:

$$\mathrm{i}(\lambda-1)\left\{\mathbf{g}_1+\left[-\mathbf{I}\quad \mathbf{B}_{12}^{(1)}\left(\mathbf{B}_{22}^{(1)}\right)^{-1}\right]\mathbf{g}_2\right\}=0 \tag{39}$$

Therefore,

$$\mathbf{g}_1=\left[\mathbf{I}\quad -\mathbf{B}_{12}^{(1)}\left(\mathbf{B}_{22}^{(1)}\right)^{-1}\right]\mathbf{g}_2\ \ (\alpha=1,2,3,4),\ \lambda_\alpha=1\ \ (\alpha=5,\ldots,8-m) \tag{40}$$

The use of Eqs. (40) and (34) and $\mathbf{d}=\mathbf{P}\mathbf{g}$ provide:

$$\mathbf{d}_1=0,\quad \mathbf{d}_2=\mathbf{W}\mathbf{g}_2 \tag{41}$$

where $\mathbf{W}=\mathbf{P}_{21}\left[\mathbf{I}\quad -\mathbf{B}_{12}^{(1)}\left(\mathbf{B}_{22}^{(1)}\right)^{-1}\right]+\mathbf{P}_{22}$, and $\mathbf{d}_1$ and $\mathbf{d}_2$ have the same dimensions as $\mathbf{g}_1$ and $\mathbf{g}_2$, respectively.

Substituting Eqs. (40) and (34) into Eq. (38) leads to:

$$\left(\lambda\mathbf{H}+\bar{\mathbf{H}}\right)\mathbf{g}_2=0 \tag{42}$$

Then the first four eigenvalues λ_1, λ_2, λ_3 and λ_4 are the roots of $\left|\lambda\mathbf{H}+\bar{\mathbf{H}}\right|=0$. The rest of the eigenvalues correspond to Eq. (40). Eq. (42) shows that $\mathbf{H}$ plays an important role in transonic and subsonic problems since it characterizes the interface and velocity behavior. After obtaining the eigenvectors $\mathbf{g}_i$, the eigenvectors $\mathbf{d}_i$ can be readily found. The eigenvector in relation to $\lambda=1$ can always be taken to be real (Shen and Nishioka, 2000).

Let $\mathbf{H}=\mathbf{E}+\mathrm{i}\mathbf{F}$, where $\mathbf{E}$ is symmetric and $\mathbf{F}$ is antisymmetric as $0\le v<v_2^{(1)}$. However, this does not hold true for a transonic crack. Therefore, Eq. (42) can be written as:

$$\mathbf{\Psi}\mathbf{g}_2=-\mathrm{i}\gamma\mathbf{g}_2 \tag{43}$$

where $\mathbf{\Psi}=\mathbf{E}^{-1}\mathbf{F}$ and $\gamma=\dfrac{1+\lambda}{1-\lambda}$.

It can be seen that if γ is an eigenvalue, then so is $-\bar{\gamma}$. γ can be determined by $\left|\mathbf{\Psi}+\mathrm{i}\gamma\right|=0$ from Eq. (43), which leads to the following fourth-order algebraic equation:

$$(\mathrm{i}\gamma)^4+a(\mathrm{i}\gamma)^3+\frac{1}{2}\left(a^2-b\right)(\mathrm{i}\gamma)^2+\frac{1}{3}\left(\frac{1}{2}a^3-\frac{3}{2}ab+c\right)(\mathrm{i}\gamma)+d=0 \tag{44}$$

where

$$a=\mathrm{tr}\left(\mathbf{\Psi}\right),\ \ b=\mathrm{tr}\left(\mathbf{\Psi}^2\right),\ \ c=\mathrm{tr}\left(\mathbf{\Psi}^3\right),\ \ d=\left|\mathbf{\Psi}\right| \tag{45}$$

The singularity of the crack-tip is defined by the roots of Eq. (44).

For $0 \le v < v_2^{(1)}$, i.e., $m = 0$, $a = c = 0$ and $d \le 0$. Hence, Eq. (44) is reduced to:

$$\gamma^4 + \frac{1}{2} b \gamma^2 + d = 0 \tag{46}$$

which has the same form as the result in Li and Kardomateas (2007).

The analytic function $\mathbf{h}(z)$ can be expanded in terms of the eigenvectors

$$\mathbf{h}(z) = \left[\mathbf{d}_1 \quad \mathbf{d}_2 \quad \cdots \quad \mathbf{d}_n \right] \cdot \left[h_1(z) \quad h_2(z) \quad \cdots \quad h_n(z) \right]^{\mathrm{T}} \tag{47}$$

where $h_i(z)$ $(i = 1, 2, \ldots, n)$ is an analytic cut along the crack surface, and $n = 8 - m$. Substituting Eq. (46) into Eq. (32) and using Eq. (35) provide:

$$\begin{cases} \lambda_\alpha h_\alpha^+(x_1) - h_\alpha^-(x_1) = 0, & \alpha = 1, 2, 3, 4 \\ h_\alpha^+(x_1) - h_\alpha^-(x_1) = 0, & \alpha = 5, \ldots, n \end{cases}, \quad x_1 < 0 \tag{48}$$

This constitutes n Riemann-Hilbert problems. Considering that the generalized displacements are bounded at the crack tip, or $|h_n(z)| = 0$ $\left(|z|^\beta\right)$ for $\beta > -1$ obtains (Shen and Nishioka, 2000):

$$\begin{cases} h_\alpha(z) = l_\alpha(z) z^{-q_\alpha}, & \alpha = 1, 2, 3, 4 \\ h_\alpha(z) = l_\alpha(z), & \alpha = 5, \ldots, n \end{cases} \tag{49}$$

where $l_\alpha(z)$ is the arbitrary entire function and analytic in the entire plane, and

$$q_\alpha = \frac{\ln \lambda_\alpha}{2\pi \mathrm{i}} \tag{50}$$

where $\mathrm{Re}(\lambda_\alpha) < 1$ since the generalized displacements are bounded at the crack tip. The eigenvalues $\lambda_\alpha = 1$ $(\alpha = 5, \ldots, n)$ give the entire function $l_\alpha(z)$ which does not cause a singularity around the crack tip. For the propagation of a subsonic crack in an anisotropic MEE bimaterial, i.e., $0 \le v < v_2^{(\mathrm{I})}$,

$$q_{1,2} = \frac{1}{2} \pm \mathrm{i}\varepsilon_1, \quad q_{3,4} = \frac{1}{2} \pm \mathrm{i}\varepsilon_2 \tag{51}$$

where

$$\varepsilon_i = \frac{1}{2\pi}\ln\frac{1-\gamma_i}{1+\gamma_i} \tag{52}$$

and γ_i is determined from Eq. (46), which is the same as that in Li and Kardomateas (2007) for the static fracture analysis of anisotropic MEE bimaterials. Note that for transversely isotropic MEE bimaterials, $\varepsilon_2 = 0$ holds true (Herrmann et al., 2010; Feng et al., 2012).

Then

$$\mathbf{M}^{-1} = \hat{\mathbf{M}} = \begin{bmatrix} \hat{\mathbf{M}}_{11} & \hat{\mathbf{M}}_{12} \\ \hat{\mathbf{M}}_{21} & \hat{\mathbf{M}}_{22} \end{bmatrix} \tag{53}$$

is introduced, where $\hat{\mathbf{M}}_{ij}$ has the same dimensions as $\mathbf{P}_{ij}$. Now, the singular terms in Eqs. (47) and (49) are considered,

$$\mathbf{f}_1'^{(1)}(z) = \hat{\mathbf{M}}_{12}\mathbf{W}\mathbf{G}\mathrm{diag}\left[z^{-q_1} \quad z^{-q_2} \quad z^{-q_3} \quad z^{-q_4}\right]\mathbf{G}^{-1}\mathbf{L},\ x_3 > 0 \tag{54a}$$

$$\bar{\mathbf{f}}'^{(2)}(z) = \hat{\mathbf{M}}_{22}\mathbf{W}\mathbf{G}\mathrm{diag}\left[z^{-q_1} \quad z^{-q_2} \quad z^{-q_3} \quad z^{-q_4}\right]\mathbf{G}^{-1}\mathbf{L},\ x_3 > 0 \tag{54a}$$

and

$$\bar{\mathbf{f}}_1'^{(1)}(z) = \bar{\hat{\mathbf{M}}}_{12}\mathbf{W}\mathbf{G}\mathrm{diag}\left[z^{-q_1} \quad z^{-q_2} \quad z^{-q_3} \quad z^{-q_4}\right]\mathbf{G}^{-1}\mathbf{L},\ x_3 > 0 \tag{55a}$$

$$\mathbf{f}'^{(2)}(z) = \bar{\hat{\mathbf{M}}}_{22}\mathbf{W}\mathbf{G}\mathrm{diag}\left[z^{-q_1} \quad z^{-q_2} \quad z^{-q_3} \quad z^{-q_4}\right]\mathbf{G}^{-1}\mathbf{L},\ x_3 > 0 \tag{55a}$$

where $\mathbf{L} = \left[l_{10} \quad l_{20} \quad l_{30} \quad l_{40}\right]^{\mathbf{T}}$ and $\mathbf{G} = \left[\mathbf{g}_{21} \quad \mathbf{g}_{22} \quad \mathbf{g}_{23} \quad \mathbf{g}_{24}\right]^{\mathbf{T}}$. The quantity l_{i0} represents the asymptotic field magnitude and depends on the external loading and geometry.

In order to avoid solving the eigenvalue problem in Eq. (43), the following expression is introduced (Shen et al., 2000):

$$\mathbf{G}\mathrm{diag}\left[\xi_1 \quad \xi_2 \quad \xi_3 \quad \xi_4\right]\mathbf{G}^{-1} = \mathbf{\Omega}_i\xi_i \tag{56}$$

where ξ_i is an arbitrary function with respect to z, and

$$\mathbf{\Omega}_1=\frac{1}{(\gamma_1-\gamma_4)(\gamma_1-\gamma_3)(\gamma_1-\gamma_2)}\left[-\mathrm{i}\mathbf{\Psi}^3+(\gamma_2+\gamma_3+\gamma_4)\mathbf{\Psi}^2+\mathrm{i}(\gamma_2\gamma_3+\gamma_2\gamma_4+\gamma_3\gamma_4)\mathbf{\Psi}-\gamma_2\gamma_3\gamma_4\mathbf{I}\right] \quad (57a)$$

$$\mathbf{\Omega}_2=\frac{1}{(\gamma_2-\gamma_4)(\gamma_2-\gamma_3)(\gamma_2-\gamma_1)}\left[-\mathrm{i}\mathbf{\Psi}^3+(\gamma_1+\gamma_3+\gamma_4)\mathbf{\Psi}^2+\mathrm{i}(\gamma_1\gamma_3+\gamma_1\gamma_4+\gamma_1\gamma_2)\mathbf{\Psi}-\gamma_1\gamma_3\gamma_4\mathbf{I}\right] \quad (57b)$$

$$\mathbf{\Omega}_3=\frac{1}{(\gamma_3-\gamma_4)(\gamma_3-\gamma_1)(\gamma_3-\gamma_2)}\left[-\mathrm{i}\mathbf{\Psi}^3+(\gamma_2+\gamma_1+\gamma_4)\mathbf{\Psi}^2+\mathrm{i}(\gamma_2\gamma_1+\gamma_2\gamma_4+\gamma_1\gamma_4)\mathbf{\Psi}-\gamma_2\gamma_4\gamma_1\mathbf{I}\right] \quad (57c)$$

$$\mathbf{\Omega}_4=\frac{1}{(\gamma_4-\gamma_1)(\gamma_4-\gamma_3)(\gamma_4-\gamma_2)}\left[-\mathrm{i}\mathbf{\Psi}^3+(\gamma_2+\gamma_3+\gamma_1)\mathbf{\Psi}^2+\mathrm{i}(\gamma_2\gamma_3+\gamma_2\gamma_1+\gamma_3\gamma_1)\mathbf{\Psi}-\gamma_2\gamma_3\gamma_1\mathbf{I}\right] \quad (57d)$$

Therefore, Eqs. (54) and (55) can be written as:

$$\mathbf{f}_1'^{(1)}(z)=z^{-q_i}\hat{\mathbf{M}}_{12}\mathbf{W}\mathbf{\Omega}_i\mathbf{L},\ x_3>0 \quad (58a)$$

$$\mathbf{f}'^{(2)}(z)=z^{-q_i}\bar{\hat{\mathbf{M}}}_{22}\mathbf{W}\mathbf{\Omega}\mathbf{L},\ x_3<0 \quad (58b)$$

and

$$\mathbf{f}_1^{(1)}(z)=z^{1-q_i}\hat{\mathbf{M}}_{12}\mathbf{W}\mathbf{\Phi}_i\mathbf{L},\ x_3>0 \quad (59a)$$

$$\mathbf{f}^{(2)}(z)=z^{1-q_i}\bar{\hat{\mathbf{M}}}_{22}\mathbf{W}\mathbf{\Phi}\mathbf{L},\ x_3<0 \quad (59b)$$

where $\mathbf{\Phi}=\frac{1}{1-q}\mathbf{\Omega}$.

Using Eqs. (24), (28) and (29) provides:

$$\mathbf{f}_2'^{(1)}(z)=\frac{1}{2}\left[\mathbf{N}_1+\mathbf{N}_2H(z)\right]z^{-q_i}\mathbf{W}\mathbf{\Omega}_i\mathbf{L} \quad (60)$$

$$\mathbf{f}_2^{(1)}(z)=\frac{1}{2}\left[\mathbf{N}_1+\mathbf{N}_2H(z)\right]z^{1-q_i}\mathbf{W}\mathbf{\Phi}_i\mathbf{L} \quad (61)$$

where $H(z)$ is the Heaviside step function and

$$\mathbf{N}_1=-\left(\mathbf{B}_{22}^{(1)}\right)^{-1}\left(\mathbf{B}_{21}^{(1)}\hat{\mathbf{M}}_{12}+\bar{\mathbf{B}}_{21}^{(1)}\bar{\hat{\mathbf{M}}}_{12}\right),\ \mathbf{N}_2=\left(\mathbf{B}_{22}^{(1)}\right)^{-1}\left\{\begin{bmatrix}\mathbf{B}_{21}^{(2)} & \mathbf{B}_{22}^{(2)}\end{bmatrix}\bar{\hat{\mathbf{M}}}_{22}+\begin{bmatrix}\bar{\mathbf{B}}_{21}^{(2)} & \bar{\mathbf{B}}_{22}^{(2)}\end{bmatrix}\hat{\mathbf{M}}_{22}\right\} \quad (62)$$

$\mathbf{N}_1$ and $\mathbf{N}_2$ are real matrices. It is noted that after the determination of $\mathbf{f}(z)$, the field quantities in Eqs. (12) and (13) can be evaluated by using a replacement of z_s for each component function. Taking into account that $\mathbf{f}_2'^{(1)}(z)$ is real, Eq. (60) leads to:

$$x^{-q_i}\mathbf{W}\boldsymbol{\Omega}_i\mathbf{L}=x^{-\bar{q}_i}\bar{\mathbf{W}}\bar{\boldsymbol{\Omega}}_i\bar{\mathbf{L}} \tag{63}$$

where x is an arbitrary real number.

Once $\mathbf{f}(z)$ is determined, the complete field of generalized stresses in the vicinity of the crack tip can be evaluated by using Eq. (13), which takes the form (Shen et al., 2000):

$$\mathbf{t}_1^{(1)}=2\,\mathrm{Re}\left[\mathbf{B}_{11}^{(1)}\left(\mathbf{Z}_1^{(1)}\right)^{-q_i}\hat{\mathbf{M}}_{12}\mathbf{W}\boldsymbol{\Omega}_i\mathbf{L}\right]+\mathbf{B}_{12}^{(1)}\left(\mathbf{Z}_2^{(1)}\right)^{-q_i}\left(\mathbf{N}_1+\boldsymbol{\Theta}\mathbf{N}_2\right)\mathbf{W}\boldsymbol{\Omega}_i\mathbf{L} \tag{64a}$$

$$\mathbf{t}_2^{(1)}=2\,\mathrm{Re}\left[\mathbf{B}_{21}^{(1)}\left(\mathbf{Z}_1^{(1)}\right)^{-q_i}\hat{\mathbf{M}}_{12}\mathbf{W}\boldsymbol{\Omega}_i\mathbf{L}\right]+\mathbf{B}_{22}^{(1)}\left(\mathbf{Z}_2^{(1)}\right)^{-q_i}\left(\mathbf{N}_1+\boldsymbol{\Theta}\mathbf{N}_2\right)\mathbf{W}\boldsymbol{\Omega}_i\mathbf{L} \tag{64b}$$

and

$$\mathbf{t}^{(2)}=2\,\mathrm{Re}\left[\mathbf{B}^{(2)}\left(\mathbf{Z}^{(2)}\right)^{-q_i}\bar{\hat{\mathbf{M}}}_{22}\mathbf{W}\boldsymbol{\Omega}_i\mathbf{L}\right] \tag{65}$$

where

$$\boldsymbol{\Theta}=\mathrm{diag}\left[H\left(z_{4-m+1}^{(1)}\right)\quad\cdots\quad H\left(z_4^{(1)}\right)\right],\ \mathbf{p}_1^{(1)}=\mathrm{diag}\left[p_1^{(1)}\quad\cdots\quad p_{4-m}^{(1)}\right] \tag{66a}$$

$$\mathbf{p}_2^{(1)}=\mathrm{diag}\left[p_{4-m+1}^{(1)}\quad\cdots\quad p_4^{(1)}\right],\ \mathbf{Z}_1^{(1)}=\mathrm{diag}\left[z_1^{(1)}\quad\cdots\quad z_{4-m}^{(1)}\right],\ \mathbf{Z}_2^{(1)}=\mathrm{diag}\left[z_{4-m1}^{(1)}\quad\cdots\quad z_4^{(1)}\right] \tag{66b}$$

$$\mathbf{p}^{(2)}=\mathrm{diag}\left[p_1^{(2)}\quad\cdots\quad p_4^{(2)}\right],\ \mathbf{Z}^{(2)}=\mathrm{diag}\left[z_1^{(2)}\quad\cdots\quad z_4^{(2)}\right] \tag{66c}$$

Then, the generalized displacements in the vicinity of the crack tip are presented as:

$$\mathbf{U}_1^{(1)}=2\,\mathrm{Re}\left[\mathbf{A}_{11}^{(1)}\left(\mathbf{Z}_1^{(1)}\right)^{1-q_i}\hat{\mathbf{M}}_{12}\mathbf{W}\boldsymbol{\Phi}_i\mathbf{L}\right]+\mathbf{A}_{12}^{(1)}\left(\mathbf{Z}_2^{(1)}\right)^{1-q_i}\left(\mathbf{N}_1+\boldsymbol{\Theta}\mathbf{N}_2\right)\mathbf{W}\boldsymbol{\Phi}_i\mathbf{L} \tag{67a}$$

$$\mathbf{U}_2^{(1)}=2\,\mathrm{Re}\left[\mathbf{A}_{21}^{(1)}\left(\mathbf{Z}_1^{(1)}\right)^{1-q_i}\hat{\mathbf{M}}_{12}\mathbf{W}\boldsymbol{\Phi}_i\mathbf{L}\right]+\mathbf{A}_{22}^{(1)}\left(\mathbf{Z}_2^{(1)}\right)^{1-q_i}\left(\mathbf{N}_1+\boldsymbol{\Theta}\mathbf{N}_2\right)\mathbf{W}\boldsymbol{\Phi}_i\mathbf{L} \tag{67b}$$

and

$$\mathbf{U}^{(2)}=2\,\mathrm{Re}\left[\mathbf{A}^{(2)}\left(\mathbf{Z}^{(2)}\right)^{1-q_i}\bar{\hat{\mathbf{M}}}_{22}\mathbf{W}\boldsymbol{\Phi}_i\mathbf{L}\right] \tag{68}$$

The most singular terms in Eqs. (64) and (65) and Eqs. (67) and (68) are dependent on the maximum of the real part of q_i, which plays a dominant role in the evaluation of the singularity at crack-tip herein. If $\mathrm{Re}(q_k)$ is the maximum, then $\boldsymbol{\Omega}_i=\boldsymbol{\Omega}_i=0$ $(i=1,2,3,4$ and $i\neq k)$ can be

taken in the aforementioned expressions. According to these equations, the generalized stress fields are singular, not only around the crack tip, but also for all of the rays that emanate from the crack tip $x_1 + p_\alpha^{(1)} x_3 = 0 \ (\alpha = 4 - m + 1, \ldots, 4)$. This means that there are shock waves that emanate from the transonic propagation of the crack tip. Additionally, for complex singularity, the generalized stress fields are also oscillatory around the angle $\theta_\alpha = 90^\circ + \tan^{-1} p_\alpha^{(1)} \ (\alpha = 4 - m + 1, \ldots, 4)$ (Shen et al., 2000).

Also, when $v < v_2^{(1)}$, $m = 0$, and

$$\mathbf{V} = \begin{bmatrix} \mathbf{B}^{(1)} & 0 \\ 0 & \bar{\mathbf{B}}^{(2)} \end{bmatrix}, \ \mathbf{M} = \mathrm{i} \begin{bmatrix} \mathbf{B}^{(1)} & -\bar{\mathbf{B}}^{(2)} \\ \mathbf{A}^{(1)} & -\bar{\mathbf{A}}^{(2)} \end{bmatrix}, \ \mathbf{W} = \mathbf{H} \tag{69}$$

The corresponding solution is reduced to:

$$\mathbf{f}^{(1)}(z) = z^{1-q_k} \left(\mathbf{B}^{(1)} \right)^{-1} \mathbf{\Phi}_k \mathbf{L}, \ x_3 > 0 \tag{70a}$$

$$\mathbf{f}^{(2)}(z) = z^{1-q_k} \left(\mathbf{B}^{(2)} \right)^{-1} \bar{\mathbf{H}}^{-1} \mathbf{H} \mathbf{\Phi}_k \mathbf{L}, \ x_3 > 0 \tag{70b}$$

which have the same form as the static problem (Li and Kardomateas, 2007).

4. Effects of speed of moving crack on singular power *q*

In this section, the effect of the speed of the crack-tip on the variation of the singularity power will be discussed. The materials of the upper and lower MEE planes in the bimaterial system are $BaTiO_3$-$CoFe_2O_4$ composites which are expressed as volume fractions V_f of piezoelectric (PE) inclusion (Sih and Song, 2003) and the electromagnetic constants are taken from Li (2000). For convenience, their material properties are listed in Table 1. Table 2 presents the two critical wave speeds for the aforementioned MEE materials (Case 1) as well as the materials without a PE effect (Case 2) and/or piezomagnetic (PM) effect (Case 3). The results in Table 2 show that the

material combinations here that neglect piezoelectricity and piezomagnetics have almost no influence on v_1 , and neglecting piezomagnetics only has a slight influence on v_2. These are consistent with the observations in Shen et al. (2000) for a piezoelectric bimaterial. However, neglecting piezoelectricity has a small influence on v_2 for the two types of materials. Additionally, for the MEE bimaterials here, the critical wave speeds v_2 in relation to the materials in the upper and lower MEE planes are equal to their corresponding shear wave speeds, respectively, which are defined as $v_s = \sqrt{\mu/\rho}$ and $\mu = c_{44} + \left(\alpha_{11}h_{15}^2 - 2e_{15}h_{15}d_{11} + \mu_{11}e_{15}^2\right)\Big/\left(\mu_{11}\alpha_{11} - d_{11}^2\right)$ (Feng et al., 2009). In the following numerical results, the critical wave speeds related to Material 1 with $V_f = 0.1$, namely $v_2^{(1)}$, which is equal to its shear wave speed v_s, will be used to normalize the speed of the crack-tip.

Table 1 Material properties of $CoFe_2O_4$-$BaTiO_3$ composites (Sih and Song, 2003; Li, 2000)

(c_{ij} in 10^9 N/m^2, e_{ij} in C/m^2, α_{ij} in 10^{-10}C/Vm, h_{ij} in N/Am, μ_{ij} in 10^{-6}Ns^2/ C^2, d_{ij} in 10^{-12}Ns/ VC, ρ in kg/m^3)

	c_{11}	c_{13}	c_{33}	c_{44}	e_{15}	e_{31}	e_{33}	h_{15}	h_{31}
Material 1 (V_f=0.1)	274	161	259	45	1.16	-0.44	1.86	495	522.3
Material 2 (V_f=0.9)	178	87.2	172.8	43.2	10.44	-3.96	16.74	55.00	58.03
	h_{33}	α_{11}	α_{33}	μ_{11}	μ_{33}	d_{11}	d_{33}	ρ	
Material 1 (V_f=0.1)	629.7	11.9	13.4	531.5	142.3	1.4	1250	5372	
Material 2 (V_f=0.9)	69.97	100.9	113.5	63.5	24.7	7.0	900	5945	

Table 2 Two critical wave speeds for materials in upper and lower planes

	MEE bimaterial (Case 1)		Without PM effect (Case 2)		Without PE effect (Case 3)	
	v_2	v_1	v_2	v_1	v_2	v_1
Material 1	2947	7142	2935	7144	2912	7144
Material 2	3016	5472	3015	5473	2700	5473

The singular parameters are given in Eq. (51) for the subsonic propagation of the crack-tip. Since the $BaTiO_3$-$CoFe_2O_4$ composites are transversely isotropic, $\varepsilon_2 = 0$ holds true and only ε_1 is presented. Fig. 1 describes the variation of the oscillating index ε when the speed of the crack-tip is less than the minimum Rayleigh wave speed of the bimaterial system in the three aforementioned cases. It is demonstrated that ε increases as the speed of the crack propagation increases and tends to ∞ when v is very close to the Rayleigh wave speed $v_R^{(1)}$ of Material 1 in Cases 1 and 2, which is similar to the results in relation to elastic and piezoelectric bimaterials (Shen and Nishioka, 2000; Shen et al., 2000). Herein $v_R^{(1)}/v_2^{(1)} = 0.9354$ and 0.9351 in Cases 1 and 2, respectively, and $v_R^{(2)}/v_2^{(1)} = 0.8559$ in Case 3. Moreover, the difference in the oscillating index ε between Cases 1 and 2 is minimal, which again means that neglecting piezomagnetics has almost no influence on ε.

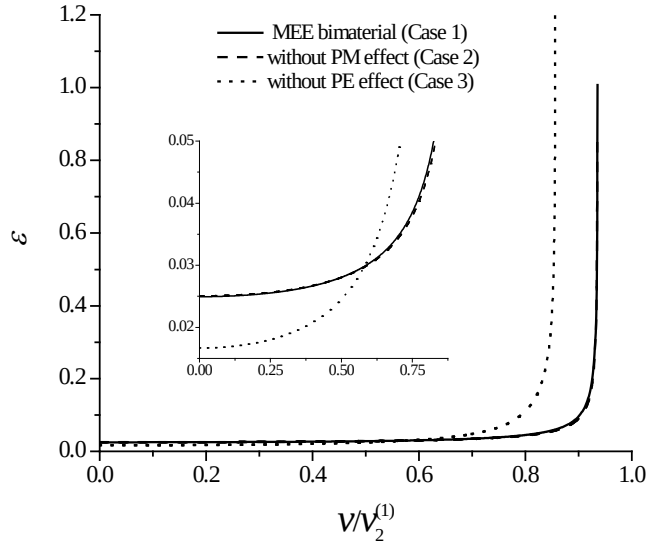

Fig. 1. Variation of the oscillating index ε with respect to normalized speed of moving crack-tip in the range $0 < v < v_R^{(1)}$

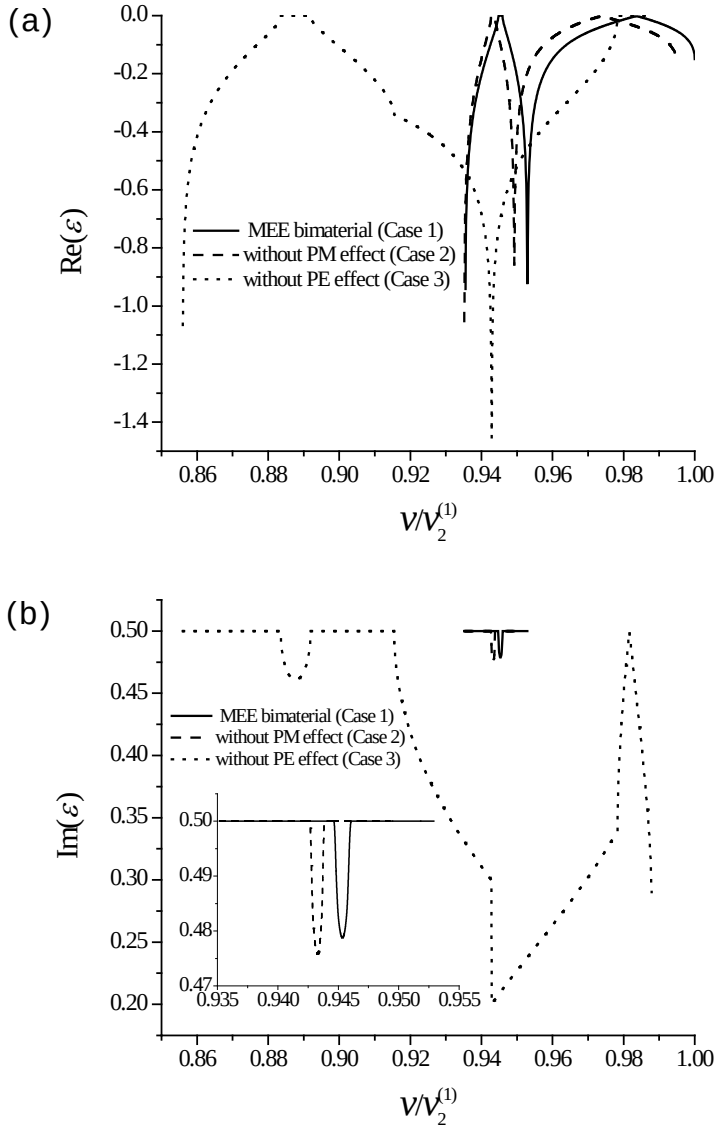

Fig. 2. Variation of the oscillating index ε_1 with respect to normalized speed of the moving crack in the range $v_R^{(1)} < v < v_2^{(1)}$ (a) Real part, (b) Imaginary part

In Fig. 2, the variation of the oscillating index ε when the speed of the crack-tip is greater than $v_R^{(1)}$ and less than $v_2^{(1)}$ in the three aforementioned cases is presented. The results in Fig. 2 show that, as the speed of the crack-tip exceeds the corresponding Rayleigh speeds, ε is no longer real and becomes complex, i.e., $\varepsilon = \mathrm{Re}(\varepsilon) + \mathrm{i}\,\mathrm{Im}(\varepsilon)$. This agrees with the conclusion in Shen et al.

(2000) in relation to piezoelectric bimaterials. However, in the work by Shen et al. (2000), the imaginary part of ε is always equal to $1/2$ as $v \in \left(v_2^{(1)}, v_1^{(1)}\right)$. In this study, the imaginary part of ε is equal to $1/2$ only in part of the interval $v \in \left(v_2^{(1)}, v_1^{(1)}\right)$ but in other parts of the interval $v \in \left(v_2^{(1)}, v_1^{(1)}\right)$ the imaginary part of ε is less than $1/2$ and even equals to zero when $v/v_2^{(1)}$ arrives at a certain value in all three cases. This is quite different from the observation by Shen et al. (2000). Moreover, as $\mathrm{Im}(\varepsilon) = \frac{1}{2}$, the real part of ε can be expressed as:

$$\mathrm{Re}(\varepsilon) = \frac{1}{2\pi} \ln \frac{\gamma - 1}{\gamma + 1} \tag{71}$$

Additionally, it is noted that the real and imaginary parts of ε related to Case 1 are very close to those related to Case 2 but not for those related to Case 3 in Fig. 2. This implies that for the MEE bimaterials in this study, neglecting the PM effect has no significant effect on ε.

Fig. 3 shows the dependence of the singularity power q with a maximum real part on the normalized speed of the moving crack-tip when the crack propagates at the interface in a transonic regime. As previously mentioned, the q with a maximum real part defines the most singular term in Eqs. (64)-(68) and plays a dominant role in the evaluation of the singularity at crack-tip. It is seen that the order of $\mathrm{Re}(q)$ is equal or extremely close to $\frac{1}{2}$ at the early stage of transonic propagation in all three cases. Then with increased speed of the crack-tip, $\mathrm{Re}(q)$ is monotonically decreased in Case 1, but has different tendencies in the other two cases. In Case 2, $\mathrm{Re}(q)$ is always less than $\frac{1}{2}$ for the majority of the range $v_2^{(1)} < v < v_1^{(2)}$, and in Case 3, always extremely close to $\frac{1}{2}$. Previous investigations have mentioned that when the power of singularity is less than $\frac{1}{2}$, the energy release rate will be zero and cannot be regarded as the driving force of

cracking herein (Huang et al., 1996; Shen et al., 2000; Wu, 2002). One possible explanation is that the weak singularity would still intensify the applied external loadings so that there is sufficient pressure at the crack tip to cause crack propagation.

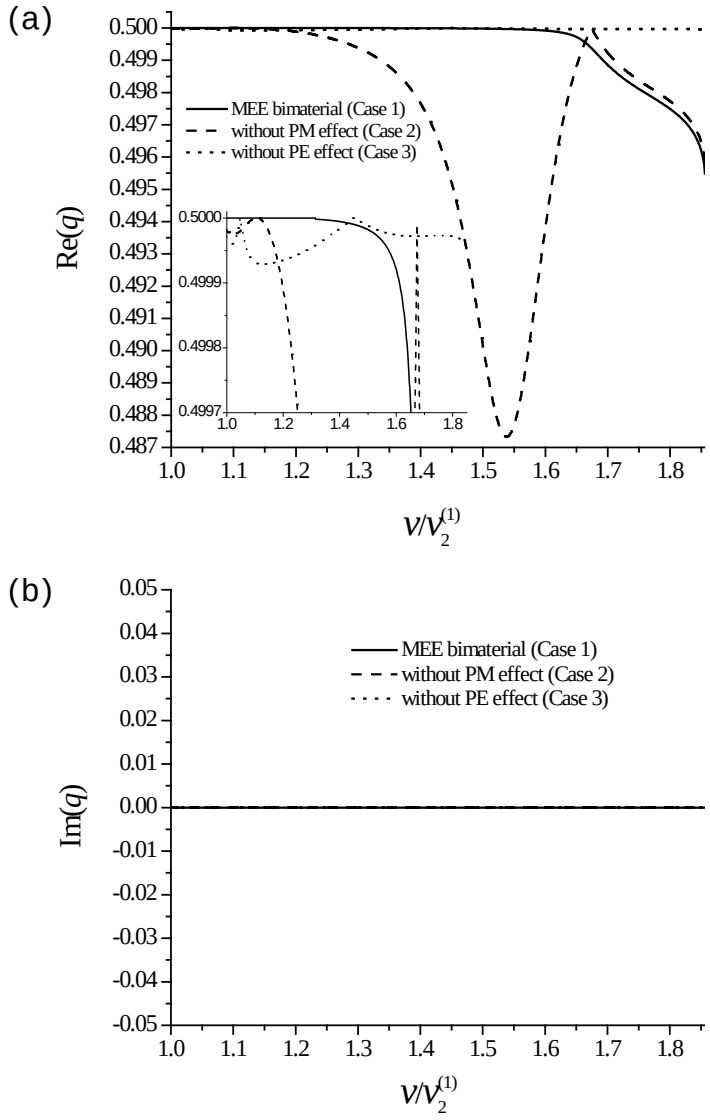

Fig. 3. Variation of singularity power q with respect to normalized speed of moving crack-tip in the range $v_2^{(1)} < v < v_1^{(2)}$ (a) Real part; (b) Imaginary part

A comparison of the results of the three cases reveals that the PM effect on $\mathrm{Re}(q)$ is very obvious for transonic propagation and the PE effect also becomes apparent at the late stages of

transonic propagation. Additionally, it is noteworthy that the imaginary part of the singularity power q for the MEE bimaterials in this study is always equal to zero for the transonic propagation in Fig. 3b, which does not agree with that observed in the piezoelectric case (Shen et al., 2000). Furthermore, the transition point of $\mathrm{Re}(q)$ with a jump of $-\frac{1}{2}$ across the maximum Rayleigh wave speed in elastic and piezoelectric bimaterials is not observed herein. This may be attributed to the similarity in the properties of the MEE materials in the upper and lower planes adopted in this work which results in similar Rayleigh wave speeds and both of them are less than $v_2^{(1)}$.

5. Conclusion

The propagation of subsonic and transonic cracks along the interfaces of MEE bimaterials is studied. The theoretical analysis indicates that the matrix **H** plays an important role in subsonic and transonic problems. For subsonic crack propagation, **H** is a Hermitian matrix, and the singularity power $q=\frac{1}{2}\pm \mathrm{i}\varepsilon_i$, where ε_i is associated with both v and the properties of the bimaterial system. For the MEE bimaterials in this study, the PM effect on ε is minimal in the subsonic regime. However, for transonic propagation, **H** is an arbitrary complex matrix and the real part of the singularity power, i.e., $\mathrm{Re}(q)$ appears to be less than $\frac{1}{2}$. There is therefore an obvious PM effect on $\mathrm{Re}(q)$.

The asymptotic results show that remote loading only influences the generalized stress magnitude around the crack tip. For transonic crack propagation, the generalized stress fields are singular not only in the vicinity of the crack tip but also for all of the rays that emanate from the crack tip $x_1+p_\alpha^{(1)}x_3=0\ (\alpha=4-m+1,\ldots,4)$. Analogous with the elastic and piezoelectric bimaterial

systems, this means that there is a Mach wave which emanates from the crack tip and moves with the crack tip.

Acknowledgement

Support from the General Research Fund of Hong Kong (HKU 17223916), the National Natural Science Foundation of China (Grant Nos. 11572358, 10772123 and 11072160) and the Training Program for Leading Talent in University Innovative Research Team in Hebei Province (LJRC006) is gratefully acknowledged.

References

Barras, F.., Kammer, D.S., Geubelle, P.H., Molinari, J.F. (2014). A study of frictional contact in dynamic fracture along bimaterial interfaces. Int J Fract, 189(2), 149-162.

Chen, X. (2009). Energy release rate and path-independent integral in dynamic fracture of magneto-electro-thermo-elastic solids. Int J Solids Struct, 46, 2706–2711.

Chen, H.S., Wei, W.Y., Liu, J.X., Fang, D.N. (2012). Propagation of a Mode-III interfacial crack in a piezoelectric-piezomagnetic bi-material. Int J Solids Struct, 49, 2547–2558.

Feng, W.J., Li, Y.S., Xu, Z.H. (2009). Transient response of an interfacial crack between dissimilar magnetoelectroelastic layers under magnetoelectromechanical impact loadings: Mode-I problem. Int J Solids Struct, 46, 3346–3356.

Feng, W.J., Su, R.K.L., Liu, J.X., Li, Y.S. (2010). Fracture analysis of bounded magnetoelectroelastic layers with interfacial cracks under magnetoelectro-mechanical loads: plane problem. J Intel Mater Syst Struct, 21(6), 581–594.

Feng, W.J., Ma, P., Su, R.K.L. (2012). An electrically impermeable and magnetically permeable interface crack with a contact zone in magnetoelectroelastic bimaterials under a thermal flux and magnetoelectromechanical loads. Int J Solids Struct, 49(23-24), 3472–3483.

Gao, C.F., Noda, N. (2004). Thermal-induced interfacial cracking of magnetoelectroelastic materials. Int J Eng Sci, 42(13-14), 1347–1360.

Hao, S., Liu, W.K., Klein, P.A., Rosakis, A.J. (2004). Modeling and simulation of intersonic crack growth. Int J Solids Struct, 41(7), 1773–1799.

Herrmann, K., Loboda, V., Khodanen, T. (2010). An interface crack with contact zones in a piezoelectric/piezomagnetic bimaterial, Arch Appl Mech, 80(6), 651–670.

Hu, K., Chen, Z. (2012). Pre-curving analysis of an opening crack in a magnetoelectroelastic strip under in-plane impact loadings. J Appl Phys, 112, 124911.

Hu, K., Chen, Z., Fu, J. (2015). Moving Dugdale crack along the interface of two dissimilar magnetoelectroelastic materials. Acta Mech, 226, 2065–2076.

Huang, J.H., Kuo, W.S. (1997). The analysis of piezoelectric/piezomagnetic composite materials containing ellipsoidal inclusions. J Appl Phys, 81, 1378–1386.

Huang, Y., Liu, C., Rosakis, A.J. (1996). Transonic crack growth along a bimaterial interface: an investigation of the asymptotic structure of near-tip fields. Int J Solids Struct, 33, 2625–2645.

Huang, Y., Wang, W., Liu, C., Rosakis, A.J. (1998). Intersonic crack growth in bimaterial interfaces: an investigation of crack face contact. J Mech Phys Solids, 46, 2233–2259.

Huang, G.Y., Wang, B.L., Mai, Y.W. (2009). Effect of interfacial cracks on the effective properties of magnetoelectroelastic composites. J Intel Mater Syst Struct, 20(8), 963–968.

Lambros, J., Rosakis, A.J. (1995). Shear dominated transonic crack growth in bimaterials — Part I: experimental observations. J Mech Phys Solids, 43, 169–188.

Li, J.Y. (2000). Magnetoelectroelastic multi-inclusion and inhomogeneity problems and their applications in composite materials. Int J Eng Sci, 38, 1993-2011.

Li, R., Kardomateas, G.A. (2007). The mixed Mode I and II interface crack in piezoelectromagneto-elastic anisotropic bimaterials. ASME J Appl Mech, 74(4), 614–627.

Liu, C., Lambros, J., Rosakis, A.J. (1993). Highly transient elastodynamic crack growth in a bimaterial interface: higher order asymptotic analysis and optical experiments. J Mech Phys Solids, 41, 1887–1954.

Liu, C., Huang, Y., Rosakis, A.J. (1995). Shear dominated transonic crack growth in bimaterials — II: asymptotic fields and favorable velocity regimes. J Mech Phys Solids, 43, 189–206.

Ma, P., Feng, W.J., Su, R.K.L. (2013). Pre-fracture zone model on electrically impermeable and magnetically permeable interface crack between two dissimilar magnetoelectroelastic materials. Eng Fract Mech, 102, 310–323.

Ma, P., Su, R.K.L., Feng, W.J. (2015). A new extended pre-fracture zone model for a limited permeable crack in an interlayer between magnetoelectroelastic materials. Acta Mech, 226, 1045–1065.

Ma. P., Su, R.K.L., Feng, W.J. (2016). Integral identities based on symmetric and skew-symmetric weight functions for a semi-infinite interfacial crack in anisotropic magnetoelectroelastic biomaterials. Int J Solids Struct, 88-89, 178–191.

Ma, P., Su, R.K.L., Feng, W.J. (2017). Moving crack with a contact zone at interface of magnetoelectroelastic bimaterial. Eng Fract Mech, 181, 143–160.

Needleman, A., Rosakis, A.J. (1999). The effect of bond strength and loading rate on the conditions governing the attainment of intersonic crack growth along interfaces. J Mech Phys Solids, 47(12), 2411–2449.

Nishioka, T., Yasin, A. (1999). The dynamic J integral, separated dynamic J integrals and moving finite element simulations for subsonic, transonic and supersonic interfacial crack propagation. JSME Int. J. Series A, 42, 25–39.

Rosakis, A.J., Samudrala, O., Singh, R.P., Shukla, A. (1998). Intersonic crack propagation in bimaterila systems. J Mech Phys Solids, 46, 1789–1813.

Samudrala, O., Rosakis, A.J. (2003). Effect of loading and geometry on the subsonic/intersonic transition of a biomaterial interface crack. Eng Fract Mech, 70(2), 309-337.

Shen, S., Nishioka, T. (2000). A unified method for subsonic and intersonic crack growth along an anisotropic bimaterial interface. J Mech Phys Solids, 48(11), 2257–2282.

Shen, S., Nishioka, T., Hu, S.L. (2000). Crack propagation along the interface of piezoelectric bimaterial. Theor Appl Fract Mech, 34, 185–203.

Sih, G.C., Song, Z.F. (2003). Magnetic and electric poling effects associated with crack growth in $BaTiO_3$-$CoFe_2O_4$ composite. Theor Appl Fract Mech, 39, 209–227.

Slepyan, L.I. (1993). Principle of maximum energy dissipation rate in crack dynamics. J Mech Phys Solids, 41, 1019–1034.

Slepyan, L.I. (2002). Models and phenomena in fracture mechanics. Springer-Verlag Berlin Heidelberg.

Wang, W., Huang, Y., Rosakis, A.J., Liu, C. (1998). Effect of elastic mismatch in intersonic crack propagation along a bimaterial. Eng Fract Mech, 61, 471–485.

Wu, J. (2002). Crack-tip field of a supersonic bimaterial interface crack. ASME J Appl Mech, 69, 693–696.

Xu, X.P., Needleman, A. (1996). Numerical simulations of dynamic crack growth along an interface. Int J Fract, 74(4), 289–324.

Yang, W., Suo, Z., Shih, C.F. (1991). Mechanics of dynamic debonding. Proc R Soc Lond A, 433, 679–697.

Yoffe, E.H. (1951). The moving Griffith crack. Philos Mag, 42, 739–750.

Yu, H., Yang, W. (1995). Mechanics of transonic debonding of a bimaterial interface: the in-plane case. J Mech Phys Solids, 43, 207–232.

Zhong, X.C., Li, X.F. (2006). A finite length crack propagating along the interface of two dissimilar magnetoelectroelastic materials. Int J Eng Sci, 44, 1394–1407.

Zhong, X.C., Liu, F., Li, X.F. (2009). Transient response of a magnetoelectroelastic solid with two collinear dielectric cracks under impacts. Int J Solids Struct, 46, 2950–2958.